ACS APPLIED ENERGY MATERIALS

www.acsaem.org Article

Water-Induced Fine-Structure Disorder and Its Effect on the Performance of Photoelectrodes in Dye-Sensitized Solar Cells

Alfredo Romero-Contreras,* Juan S. Lezama Pacheco, Joaquin Alvarado, Umapada Pal, and Julio Villanueva-Cab*

Cite This: *ACS Appl. Energy Mater.* 2022, 5, 4817−4828 Read Online

ACCESS | Metrics & More | Article Recommendations

ABSTRACT: Water incorporation in an electrolyte solution has become a popular method for increasing the photoconversion efficiency (PCE) of dye-sensitized solar cells (DSSCs). Although the PCE enhancement in DSSCs has been associated with incorporation of a precise amount of water, the fundamental mechanisms underlying such an enhancement remain unclear. Enhanced photocurrent in aqueous electrolyte DSSCs has also been linked to band-edge shifting, which leads to higher electron injection efficiencies. From X-ray absorption fine-structure spectroscopy (XAFS) of TiO_2 electrodes of dismantled DSSCs and electrodynamical characterization of the assembled aqueous DSSCs, we show that a less static disordered (lowest Debye−Waller value) and more relaxed lattice (interatomic distances comparable to bulk TiO_2) are the fingerprints for the optimized aqueous DSSC. On the other hand, lower efficiency of aqueous DSSCs is associated with a more static disordered (higher Debye−Waller values compared to the optimal aqueous DSSC) and less relaxed lattice (lower interatomic distances compared to bulk TiO_2). For the optimum amount of water, small perturbation-based stepwise light-induced transient measurements of the photocurrent of the operational DSSCs revealed a decrease in the overall trap density in the intragap states of the TiO_2 electrode. The decrease in intragap states induces a downward shift of the quasi-Fermi level, which is responsible for the short-circuit photocurrent amplification. The findings of this study establish a direct link between the structural parameters such as the interatomic distance and the Debye−Waller factor with electrodynamical and photovoltaic parameters such as the total trap density and PCE for the electrodes used in aqueous DSSCs, paving the way for research into more stable and environmentally friendly solar cells.

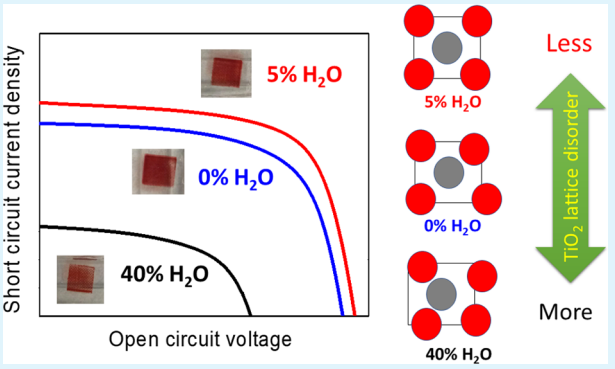

KEYWORDS: *X-ray absorption fine-structure spectroscopy, TiO_2 electrodes, X-ray absorption, DSSC performance, electrodynamical parameters*

1. INTRODUCTION

Dye-sensitized solar cells (DSSCs) have received substantial research attention during the past two decades because of their several advantages over conventional photovoltaic (PV) cells such as their simple fabrication procedure, low cost, and attractive power conversion efficiency (PCE) around 13%.[1,2] In fact, the DSSCs are an ecofriendly option for massive application and to face the current and future energy demand. A typical DSSC is an electrochemical device, composed of three essential parts: a photoanode, a counter electrode, and an electrolyte solution.[3] The photoanode is composed of a high-band-gap semiconductor (TiO_2, ZnO, etc.) layer and a screen printed over a transparent conductive oxide (TCO)-coated glass substrate, which is sensitized to visible sunlight with dye molecules responsible for solar light harvesting. The semi-transparent counter electrode is a TCO glass covered with a catalyst material, mostly platinum. Finally, the electrolyte solution is a combination of solvents containing the ions responsible for reduction/oxidation reactions, commonly I^-/I_3^- ions. The commonly used electrolyte solvents in DSSCs are volatile, flammable, and toxic, which not only have a negative environmental impact but also affect the stability of these devices. In recent years, researchers have devoted considerable efforts to replacing these commonly used electrolyte solvents with more environmentally friendly solvents, like water in DSSCs.[3−7] Water-based DSSCs promote cost reduction, nonflammability, environmental compatibility, and stability of

Received: January 21, 2022
Accepted: March 21, 2022
Published: April 4, 2022

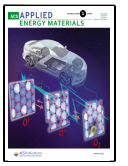

https://doi.org/10.1021/acsaem.2c00245
ACS Appl. Energy Mater. 2022, 5, 4817−4828

these PV devices.[8] Despite these advantages, utilization of water as an electrolyte solvent contributes in several ways to affect the efficiency and stability of DSSCs adversely. One common limitation of using water as an electrolyte solvent is the detachment of dye molecules from the semiconductor (TiO_2) surface, which has been associated with the competitive adsorption of water and dye molecules at the hydrophilic surface of the semiconductor.[9] Furthermore, unless the DSSCs are assembled in nonhumid conditions (which is not frequently the case), water is present during all of the fabrication steps. Therefore, the water molecules present in the ambient can be adsorbed on the semiconductor surface, be present in the solvents used to prepare the liquid electrolyte, or permeate the polymer films used for device sealing.[10,11] To understand these negative effects on the performance of DSSCs, several researchers performed studies by incorporating water in their used electrolyte solutions intentionally.[12−16] The first analytical report on this issue was published by Lindquist et al.[12] They showed that the use of water produces a negative effect on the efficiency of DSSCs due to the desorption of dye (N3) molecules from a semiconductor surface. They concluded that the competitive adsorption of water at the TiO_2 surface with the hydrophilic dye molecules is responsible for weakening the TiO_2−dye binding, which results in a reduction of the short-circuit current density (J_{SC}), which eventually affects the overall efficiency of the device. After the report of Lindquist et al., the use of hydrophobic dyes was tested by several research groups to avoid dye detachment from the semiconductor surface in the presence of water in electrolyte solvents.[13−15] The first remarkable work on this was performed by O'Regan et al.[14] They demonstrated that the presence of water does not affect the efficiency (η) and stability of DSSCs until a certain critical concentration (higher than 40% of the electrolyte volume), especially when a hydrophobic dye (TG6) is used. Subsequently, Frank et al.[15] investigated the effects of water addition in two commonly used electrolyte solvents, acetonitrile/valeronitrile (ACN/VAN) and 3-methoxypropionitrile (MPN) in combination with a hydrophobic dye (Z907). They reported that water improves the DSSC efficiency in both electrolyte configurations. The authors explained their results based on a downward shift of the conduction band of the semiconductor due to an increase in the proton concentration at the TiO_2 surface, causing an enhancement of charge collection efficiency of the photoanode and a consequent increase in the J_{SC} of the device.

Several other research groups have also demonstrated that the presence of a specific amount of water in an electrolyte solution can enhance the efficiency of DSSCs. For example, Weng and co-workers[16] observed that by increasing the water concentration up to 2.2 M, V_{OC} and the fill factor (FF) values of DSSCs increase monotonically, while J_{SC} decreases continuously. All of these observed changes are deeply rooted in a decrease in the electron injection efficiency, and the changes occur at the surface of the TiO_2 layer due to the presence of water in the electrolyte. Principal changes occurring at the surface of a TiO_2 electrode are the increase in the surface-trap state concentration, attributed to the increase of oxygen vacancies at the metal oxide structure.[17]

Recent efforts to produce DSSCs on an industrial scale have switched the attention of researchers toward aqueous DSSCs to increase the product features in terms of safety, environmental friendliness, costs, and stability. For example, Sonigara et al.[4] proposed the use of a surface-active amphiphilic quasi-solid aqueous polymer gel electrolyte (PGE) with the introduction of a hydrophobic dye (SK3) in water-based DSSCs. They found that the presence of water and chenodeoxycholic acid in the polymer matrix increases the stability of dye molecules adsorbed over the surface of a TiO_2 layer. The utilization of polymeric compounds in aqueous electrolytes is a novel and environmentally friendly option to tackle the stability issue of DSSCs. On the other hand, Fagiolari and co-workers[5] investigated the effects of polymeric (poly(ethylene oxide), poly(ethylene glycol), carboxymethyl cellulose, and xanthan gum) and molecular compound (α-terpineol, propylene carbonate) addition to a commercial TiO_2 paste. The addition of poly(ethylene glycol) in the TiO_2 paste (used for preparing the photoanode) was seen to be most beneficial, as it led to an enhancement of the short-circuit current density by about 18% and reduced the carrier recombination at the photoanode/electrolyte interface. The improvement of these characteristics of the cell resulted in an increase in the efficiency by 48% with respect to the ones prepared by TiO_2 paste without a polymeric additive (pristine). Semiconductor surface treatment has been also employed to improve the efficiency of water-based DSSCs. Kim et al.[6] reported the fabrication of such ecofriendly DSSCs based on water-containing electrolytes. For this purpose, the dye molecules were dissolved in the water-based electrolyte to be kinetically adsorbed on the surface of the TiO_2 photoanode. To improve the dye adsorption capacity and affinity of the photoanode toward a water-based electrolyte, they used a plasma treatment on its surface. The photovoltaic efficiency of the ecofriendly DSSCs fabricated using such photoanodes increased by about 3.4 times compared to the DSSC fabricated with the photoanode without plasma treatment.

After these earlier studies, the efforts to understand the collateral effects of water incorporation in DSSCs have been mainly focused on the correlation between photovoltaic and electrodynamical results. On the other hand, efforts have been devoted to engineering the processes, fabricating hydrophobic dyes, use of hydrophobic coadsorbents, etc., to make the DSSCs water-resistant as far as possible. As has been stated earlier, in most of the cases, the instability of water-based DSSCs has been associated with the change in surface characteristics of a TiO_2 photoanode, such as (1) the morphology-assisted inhibition of recombination at the electrode/electrolyte interface along with a decrease in transport resistance,[5] (2) air plasma treatment-assisted modification of the TiO_2 surface to enhance the dye attachment at its surface,[6] and (3) the inhibition of electron recombination at the TiO_2 surface through the reduction of surface-trap states.[16,17] All of these studies have shown a significant dependence of most of the photovoltaic and electrodynamical device parameters with the attenuation/modification of the TiO_2 surface due to the presence of water in an electrolyte solvent. However, to the best of our knowledge, there exists not even a single study that correlates the structural changes that occur at the TiO_2 photoanode surface due to the presence of water molecules in the electrolyte and the photovoltaic/electrodynamical parameters of the fabricated DSSC, such as its photoconversion efficiency and the electron diffusion coefficient. In the present study, we fabricated TiO_2 photoanode-based DSSCs using electrolyte solutions containing different percentages (from 0 to 40 vol %) of water to elucidate their impact on the photovoltaic performance of the devices. Optimum water content in the

https://doi.org/10.1021/acsaem.2c00245
ACS Appl. Energy Mater. 2022, 5, 4817−4828

electrolyte solution is seen to improve the short-circuit photocurrent and a significant decrease of the open-circuit photovoltage, leading to an overall increase in the photovoltaic efficiency of the fabricated DSSCs. The stepped light-induced transient measurements (SLITM) of the photovoltage and photocurrent were utilized to determine the contribution of incorporated water (into the electrolyte solution) to the electron transport time, Fermi-level shift, and oxygen vacancies (trap energies within the TiO_2 band gap) of the assembled devices. The X-ray absorption fine-structure (XAFS) technique was utilized to investigate the variation of interatomic distances of the TiO_2 photoanodes on using them in the DSSCs fabricated with water-containing electrolytes. The obtained results indicate that the enhanced performance of DSSCs fabricated with a water-containing electrolyte solution in an optimum concentration is only due to an increase in the short-circuit photocurrent. The increase in the short-circuit photocurrent is attributed to a downward shift of the conduction band of the TiO_2 electrode, as observed by SLITM measurements. The decrease in the open-circuit photovoltage is also attributed to the downward shift of the conduction band. Finally, the downward shift of the conduction band of the TiO_2 photoanode is attributed to a decrease of the oxygen vacancies of the TiO_2 electrode and a more relaxed TiO_2 lattice, as revealed by XAFS analysis.

2. MATERIALS AND METHODS

2.1. Materials. TiO_2 paste (18NR-T), transparent conducting oxide (TCO)-coated glass substrates (F-doped SnO_2; 15 Ω/sq), thermoplastic (Surlyn, Dupont), and Z907 (*cis*-bis(isothiocyanato)-(2,2′-bipyridyl-4,4′-dicarboxylato)(4,4′-di-nonyl-2′-bipyridyl)-ruthenium(II)) dye were purchased from Greatcell. 1-Butyl-3-methylimidazolium iodide, iodine, acetonitrile, valeronitrile, chloroplatinic acid (H_2PtCl_6), isopropanol, and iodine were purchased from Sigma-Aldrich, Mexico. Deionized water (18 MΩ cm at 25 °C) was obtained from a Barnstead Easypure II water purifier system.

2.2. Device Fabrication. TiO_2 films (0.25 cm^2 area) were fabricated by depositing the TiO_2 paste (18NR-T) onto TCO-coated glass substrates through screen-printing (using a 43T mesh screen). After air-drying, the deposited layers were sintered in air at 500 °C for 1 h. After cooling to 120 °C, the films were immersed into a hydrophobic dye solution (0.3 mM Z907 dye in acetonitrile/*tert*-butanol 1:1) for 16.5 h. The average thickness of the fabricated nanocrystalline TiO_2 layers was 12.3 μm with a standard deviation of ±0.26 μm (as obtained from profilometry measurements of five samples, Dektak II profilometer). The counter electrodes were prepared by spreading two drops of a 5 mM H_2PtCl_6 solution in 2-propanol over TCO-coated substrates and their subsequent firing at 450 °C for 30 min. The electrode and counter electrode were then sealed in a sandwich configuration using a 60 μm thick thermoplastic (Surlyn, Dupont) under heating. The electrolyte solution was introduced through a small hole in the predrilled counter electrodes. A vacuum system was employed to extract the air bubbles, assuring the complete penetration of the electrolyte solution into the mesoporous semiconductor structure. After the introduction of electrolyte solution into the sandwich configuration, the hole was sealed using a small piece of thermoplastic and corning glass under heating.[18] The used electrolyte contained 0.6 M 1-butyl-3-methylimidazolium iodide and 0.03 M iodine in acetonitrile/valeronitrile (85:15, v/v) with deionized water added in 0, 2, 5, 10, 20, and 40 vol %.

2.3. Device Characterization. *2.3.1. Photovoltaic Characterization.* The current density versus voltage ($J-V$) traces of the fabricated devices were recorded at room temperature, using a setup consisting of a white light-emitting diode (LED) calibrated to an irradiance of 100 mW/cm^2. The electrodes of the DSSCs were directly connected to a Keithley 2400 source meter, controlled by a free access code[19] used to extract the main parameters from the $J-V$ curves recorded under illumination.

2.3.2. Stepped Light-Induced Transient Measurements (SLITM). The SLITM of photovoltage and photocurrent were performed on the DSSCs to estimate the electron lifetime, carrier (electron) transport time, and charge density of the photoanodes, following the procedure reported earlier.[20] In brief, a stepped modulated laser-LED beam of a 630 nm wavelength (probe) superimposed on a relatively large background (bias) illumination (also a 630 nm beam) was shot over the DSSC. The modulated and the bias light entered the cells through the photoanode side. The modulated response of the DSSC, i.e., the photovoltage decay (under open-circuit conditions) or photocurrent transient (under short-circuit conditions) was recorded using a BTS1102B-EDU Tektronix oscilloscope and used to fit with a single exponential decay function with an exponent $-t/\tau_t$, where τ_t is the electron lifetime (in the case of photovoltage decay measurements) or electron transport time (in the case of photocurrent transient measurements).[21,22] The steady-state photoinjected electron density in the TiO_2 films was estimated from the relation $n = \frac{T_a J_{SC} \tau_t}{qd(1-P)}$,[20,21] where T_a is a thermodynamic factor, J_{SC} is the short-circuit photocurrent density established by the bias illumination under short-circuit conditions, P is the film porosity (P = 0.6, according to the commercial paste specifications), q is the absolute value of the electron charge, and τ_t is the electron transport time for electron density at the short circuit. The thermodynamic factor α is related to the steepness of the trap distribution or the average trap depth and related to temperature by $\alpha^{-1} = T_a/T$, where T_a is the characteristic temperature and T is the room temperature, assumed to be constant for all of the samples. The electron diffusion coefficient D was determined from the expression $D = \frac{d^2}{3.54\tau_t}$, where d is the TiO_2 film thickness (about 1.2×10^{-7} cm as measured by profilometry) and τ_t is the measured electron life or the electron transport time.[23] Neutral density filters were used to probe electrodynamical parameters of DSSCs at different intensities of illumination. For each water concentration, at least five DSSCs were fabricated. Additionally, all of the photovoltaic and electrodynamic studies were repeated five times to confirm the reproducibility of the results.

2.3.3. XAFS Characterization and Data Analysis. The coordination environment of Ti(IV) in TiO_2 photoanodes was investigated with extended X-ray absorption fine-structure (XAFS) analysis, specifically using the X-ray fluorescence technique at the Titanium k-edge absorption energy (4.996 keV). The photoanode labeled as a base was a nanocrystalline TiO_2 layer (2 μm thickness) over fluorine-doped tin oxide (FTO)-coated glass heated at 500 °C for 1 h. The photoanodes labeled 0, 5, and 40% water volume refer to the photoanodes (nanocrystalline TiO_2 layers sensitized with Z907 dye) collected by dismantling the DSSCs fabricated with electrolyte solutions containing corresponding vol % of water. For XAFS characterization, all of the photoanodes collected by disassembling the fabricated DSSCs were supported on a transparent plastic holder and measured under atmospheric conditions (25 °C, 1 atm). The XAFS measurements were repeated six times for each sample and the resulting spectra were merged using Athena software.[24] The collected XAFS data were processed and analyzed using Demeter software.[24] Phase-shift and backscattering amplitude functions (required for fitting structural models to the XAFS spectra) were calculated in FEFF using a bulk-like crystal structure of TiO_2 in the anatase phase.[25] The calculations were performed using the usual discrete form of the XAFS equation[26,27]

$$\chi(k) = \sum_j \frac{N_j}{kr_j^2} S_j^2 f_j(k) \sin\,[2kr_j + \phi(k)] \exp^{-2\sigma_j^2 k^2} \exp^{-2r_j/\lambda_j(k)} \quad (1)$$

where $f_j(k)$ and $\phi(k)$ are the effective scattering amplitude and the phase function, respectively, r_j is the distance from the absorbing atom to the nearest scattering atoms (interatomic distance), N_j is the degeneracy or the number of neighboring atoms, S_j^2 is the electronic

https://doi.org/10.1021/acsaem.2c00245
ACS Appl. Energy Mater. 2022, 5, 4817−4828

reduction factor, $\lambda_j(k)$ is the photoelectron inelastic mean free path, and σ_j^2 is the Debye−Waller factor. The XAFS Debye−Waller factor (σ_j^2), also known as the mean square relative displacement, is the square of the standard deviation of the half-path length and can be related with static and/or thermal disorder.[26,27] The Debye−Waller factor is given by eq 2

$$\sigma_j^2 = \langle (r - \bar{r})^2 \rangle \quad (2)$$

where r is the absorbing atom position and $\bar{r}$ is the position of the scattering atom; therefore, σ_j^2 has square length units.[26,27] Typical values of the σ_j^2 fall within the 0.002−0.03 Å^2 range. A larger value of σ_j^2 (beyond the 0.002−0.03 Å^2 range) would indicate that the used model is wrong or incomplete.[26] The Hanning window function was used to delimitate the fitting area in R-space from 0 to 6 Å.

3. RESULTS AND DISCUSSION

3.1. Photovoltaic Characterization. To study the effect of water incorporation into an electrolyte solution on the photovoltaic performance of DSSCs, we used a DSSC with no water (0.0 vol % water, also labeled as reference cells) and DSSCs containing different water contents (2, 5, 10, 20, and 40 vol % of water in the electrolyte solution). In Table 1, we compare the averaged photovoltaic parameters of a set of five samples of each group (i.e., the cells fabricated with the electrolyte solutions containing different water contents). As can be noticed, the short-circuit photocurrent density (J_{SC}) increased initially (up to 5%) with water content, and then reduced. The use of 2 and 5% water in the electrolyte solution enhanced J_{SC} by around 12.7% (from 10.30 to 11.80 mA/cm^2) and 18.2% (from 10.30 to 12.59 mA/cm^2), respectively. However, a further increase in water content (≥10 vol %) produces a negative effect on the J_{SC}. The J_{SC} gradually decreased from 12.59 to 1.49 mA/cm^2 on increasing water content from 5 to 40% in the electrolyte solution, which is about 88% reduction in the J_{SC} value with respect to the reference cell.

Table 1. Summary of Photovoltaic Parameters for Devices Fabricated with and without Water in the Electrolyte Solution[a]

water vol %	J_{SC} (mA/cm^2)	V_{OC} (mV)	FF (%)	η (%)
0	10.30	760.40	52.42	4.09
2	11.80	751.00	50.60	4.46
5	12.59	717.27	51.43	4.76
10	9.74	720.30	49.40	3.65
20	4.17	678.30	46.70	1.32
40	1.49	570.73	49.90	0.45

[a]Values for each parameter were estimated from the average of at least five samples.

From Table 1, it can also be observed that the V_{OC} gradually decreased from 760.40 to 570.73 mV on increasing the water content in the electrolyte solvent from 0 to 40%, representing about 25% V_{OC} decrease with respect to the reference cell. Finally, a marginal decrease of fill factor (FF) was observed on increasing the water content from 2 to 40%.

The variation of photovoltaic parameters of the fabricated DSSCs with water content in the electrolyte solution is plotted in Figure 1. It can be observed in Figure 1A that the efficiency (η) of the DSSCs reaches its highest value for 5% water content in the electrolyte. As has been stated earlier, the J_{SC} (Figure 1B) also takes its maximum value at the same water concentration. The V_{OC} gradually decreases from 760.40 to 570.73 mV on increasing the water content from 0 to 40%. The lowest V_{OC} corresponds to the device fabricated with 40% water (in the electrolyte). The observed voltage decrease was around 25% compared with the reference DSSC (Figure 1C). Finally, the fill factor (FF) did not show a significant change with water content in the electrolyte (Figure 1D). From the photovoltaic results presented above, we can conclude that efficiency variation (Figure 1A) of the devices is influenced mainly by the J_{SC} variation (Figure 1B) due to the variation of water content in the electrolyte. Despite a gradual decrease of V_{OC}, the efficiency increased around 14% when the water content in the electrolyte reached 5 vol %. In fact, such a variation of efficiency has also been observed by several research groups,[14,15] who associated such a variation mainly to the variation of J_{SC} due to the change of water content in the electrolyte.

3.2. Structural Characterization. Studies on the structural and electronic effects such as a change in the interatomic distances of TiO_2 atoms and structural disorder in a TiO_2 photoanode due to the presence of water in the electrolyte solution of DSSCs are of huge interest to understand the latest observed photovoltaic results. XAFS spectroscopy was used to study the local structural changes and short-range structure variations of the TiO_2 lattice in the photoanodes. For this purpose, photoanodes from the DSSCs that showed the highest (5 vol % water) and lowest (40 vol % water) efficiencies, a reference photoelectrode (0.0 vol % water), and a base sample (TiO_2 film not used in DSSC) were inspected. Figure 2 presents the normalized absorption spectra of the samples after postedge background subtraction. The relative heights of the pre-edge peaks (inset A in Figure 2) and the postedge features (inset B in Figure 2) are labeled according to those reported for the anatase phase.[28] The pre-edge peaks, labeled as A_1, A_2, and A_3, lie between 4.965 and 4.975 keV (inset A in Figure 2). At energy close to 4.980 keV, a shoulder was identified over the absorption edge and labeled B. The postedge peaks (X-ray absorption near-edge spectroscopy (XANES) region) are divided into two groups. The peak labeled C corresponds to the most intense peak in the near-edge XAFS spectrum and the peaks labeled D_1, D_2, and D_3 lying in-between 4.990 and 5.010 keV correspond to the fine features (inset B in Figure 2). All of these pre-edge and postedge peaks correspond to the electronic states of titanium, indicating that the anatase phase is dominating in the samples.[29,30]

To determine the structural changes in the TiO_2 lattice of the photoanodes due to water incorporation in the DSSCs, a reference structure model that corresponds to a bulk-like TiO_2 anatase phase[30] (Figure 3) was utilized. Athena and Artemis software were used to analyze and compare the XAFS data, as shown in Figure 2, with the reference model. In Figure 3, the oxygen atoms (red spheres) are surrounded by titanium atoms (gray spheres) accordingly, with the bulk TiO_2 anatase structure forming a tetragonal lattice. For identification, the atoms, as shown in Figure 3, were labeled according to their relative distance to the absorbing Ti (denoted in Figure 3) atom located at the center of the structure. The first oxygen atoms neighboring the central Ti are denoted as @O1.1 and @O1.2, and the first titanium atoms neighboring the central Ti are denoted as @Ti1.1. In a similar way, the oxygen atoms belonging to the second nearest neighborhood of the central Ti atom are denoted as @O2.1 and @O2.2, and the titanium atoms belonging to the second nearest neighborhood of the

https://doi.org/10.1021/acsaem.2c00245
ACS Appl. Energy Mater. 2022, 5, 4817−4828

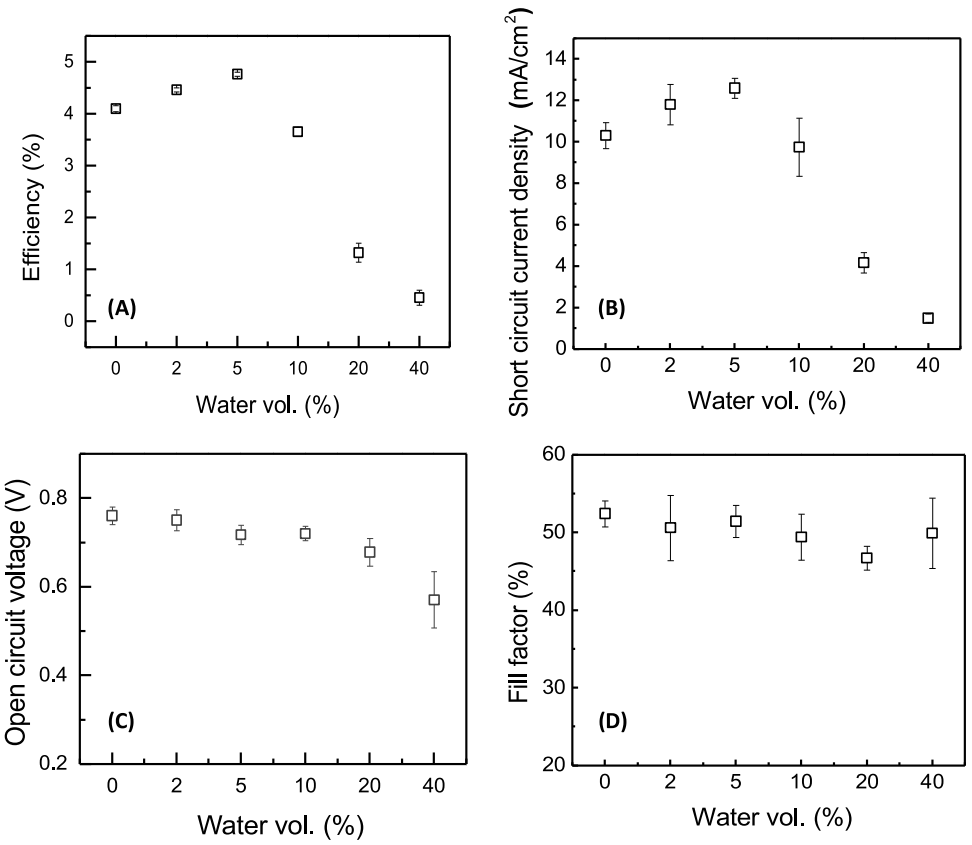

Figure 1. Effect of water content in the electrolyte solution on the photovoltaic parameters of DSSCs: (A) efficiency, (B) short-circuit photocurrent density, (C) open-circuit voltage, and (D) fill factor. The error bars correspond to the fluctuation of values in a set of five devices.

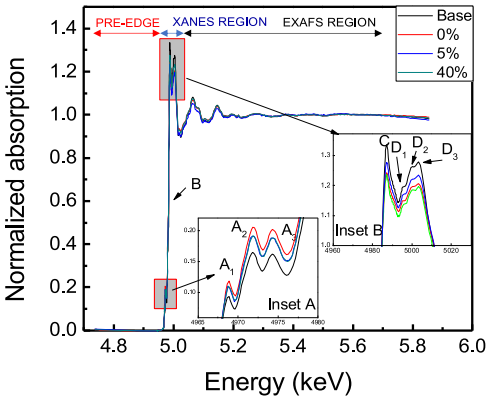

Figure 2. Normalized Ti K-edge (around 5 keV) absorption spectra of the TiO_2 photoanodes utilized in DSSCs fabricated with different water contents in electrolytes. The labeled peaks in the figure insets correspond to anatase.[29,30]

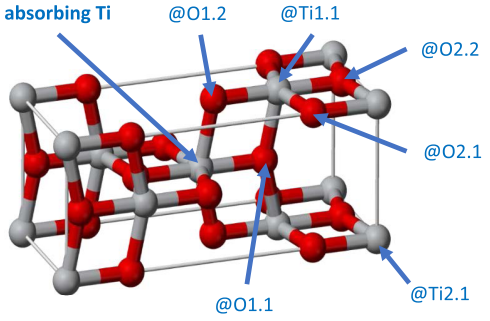

Figure 3. Schematic illustration of the reference model of bulk TiO_2 anatase utilized to determine the structural changes in the TiO_2 lattice due to water. The original image was obtained from ref 31. Copyright (2008) National Academy of Sciences, U.S.A.

central Ti atom are denoted as @Ti2.1. Knowing the relative positions of the constituent atoms from the absorbing Ti atom and the TiO_2 lattice parameters from the reference structure model (see Table 2),[29,30] we were able to obtain the variations in the interatomic distance for all of the tested samples (Figure 2). Finally, only the first four neighboring atoms were considered in the XAFS analysis.

Figure 4A,B shows the variations in the interatomic distance for the photoanodes due to water incorporation in the DSSCs obtained by fitting the spectra presented in Figure 2 with the XAFS equation (eq 1). In both graphs, the interatomic distances of the first six neighboring atoms of the reference model (Figure 3) were included for comparison. The error bars of the fitted interatomic distances represent the statistical error from six XAFS measurements of each sample.

Table 2. Summary of Interatomic Distances for the Water-Exposed Photoanodes

	interatomic distance (Å)					
sample	@O1.1	@O1.2	@Ti1.1	@O2.1	@O2.2	@Ti2.1
model	1.87	1.92	2.99	3.86	4.19	4.78
base	1.86	1.96	3.04	3.82	3.73	4.82
0%	1.87	1.92	2.99	3.85	4.19	4.78
5%	1.80	1.94	3.03	3.77	4.30	4.77
40%	1.85	1.96	3.04	3.82	3.73	4.82

https://doi.org/10.1021/acsaem.2c00245
ACS Appl. Energy Mater. 2022, 5, 4817−4828

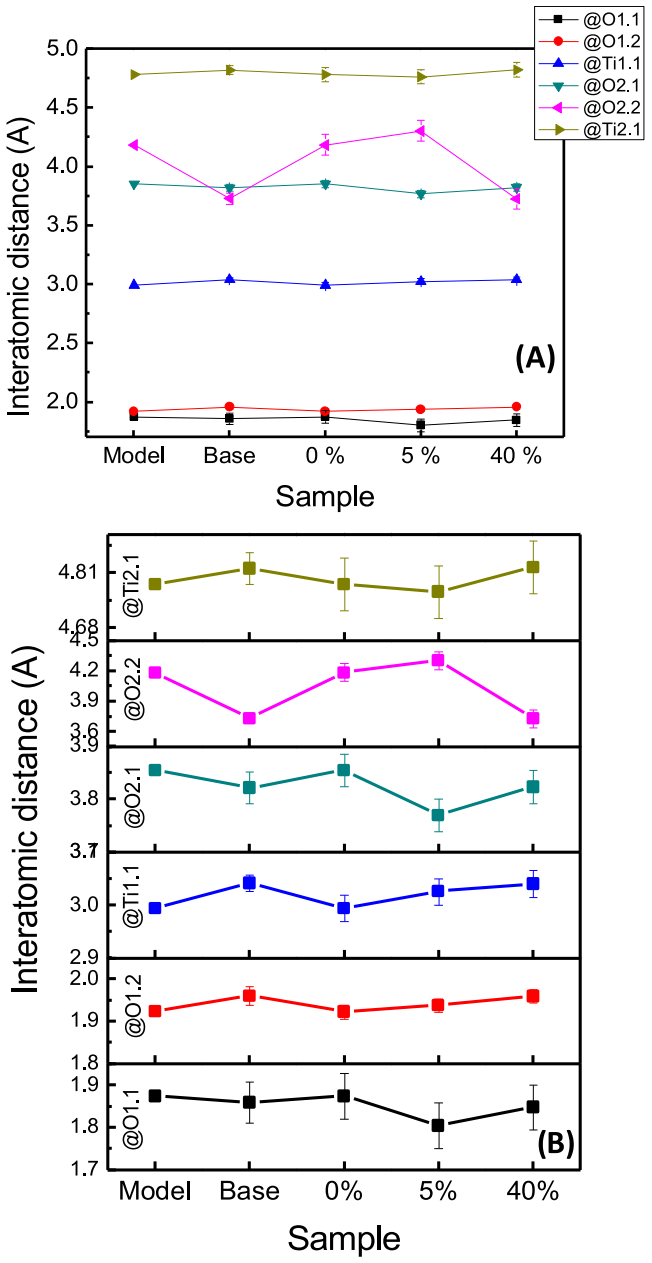

Figure 4. Variation of the interatomic distance for the first six atoms around the central/absorbing Ti atom of the TiO_2 photoanodes measured in this study. Interatomic distances for a model of bulk TiO_2 anatase are included to compare with the experimental results. (A) All of the data in the same plot and (B) same data as in (A) presented in a stack for its individual analysis.

Figure 4A shows that almost all of the atoms in the lattice have a slight variation from the model (depicted in Figure 3), but the @O2.2 atom of all of the samples suffered the most. For instance, for the base film, the distance of the @O2.2 atoms reduces from 4.185 Å (corresponding to the model) to 3.73 Å, representing a shrinkage of about 10.8% of its interatomic distance (Table 2). Such a shrinkage of the interatomic distance might be related to the presence of a significant number of oxygen vacancies at the surface of the base film, producing a notable distortion of the TiO_2 lattice. It is well known that the electronic and structural properties of a material can vary between its bulk and nanostructures.[17,32] In the present case, the available surface area in the nanostructured TiO_2 film in the base sample is around 1000 times larger than in the bulk (model); therefore, a large number of surface defects are expected. In general, the surface defects in metal oxide nanostructures such as TiO_2 are related to oxygen vacancies (energy states within the semiconductor band gap, also called trap energies), leaving most of the superficial titanium atoms with incomplete chemical bonds.[17] To compensate for this charge imbalance, the titanium atoms try to occupy lower energy sites, generating a distorted lattice and consequently, a variation in the interatomic distances between the oxygen and titanium atoms in the nanostructured sample. For the 0 vol % water-containing device, the oxygen atom (@O2.2) in the TiO_2 photoanode takes the bulk-like position, as shown in Figure 4A and Table 2. This photoanode is a sensitized TiO_2 film that was used in an ensembled device with no water in the electrolyte solution. In this photoanode, the Z907 dye molecules are attached over the TiO_2 surface through the interaction between the carboxyl groups of the dye (partially negative charged) and the oxygen vacancies of TiO_2 (partially positive charged) by electrostatic forces. Therefore, it is expected that the vacancies are filled up and the TiO_2 lattice attempts to recover its bulk-like structure.

Interestingly, the presence of 5 vol % water causes a slight shift of the @O2.2 atom from its original position (the position in bulk TiO_2). Its position changes from 4.19 Å (corresponding to the model) to 4.30 Å, representing an increase of about 2.8% on its interatomic distance (Table 2). Finally, the @O2.2 atom position for the 40 vol % water photoanode takes an interatomic distance of 3.73 Å, which is very similar to the value in the base film. This may be related to dye desorption or weakening of the bonding force between the dye molecule and the TiO_2 surface due to the presence of water at the photoanode surface. Some investigations have reported the use of protic solvents (like water) added in the electrolyte solution for DSSCs.[12,33] Their results show that the use of aqueous electrolyte solutions decreases the J_{SC} in comparison with the aprotic electrolytes (no water), and the results were explained in terms of a decrease in electron injection efficiency of dye molecules. In fact, the J_{SC} was found to decrease with irradiation time; which has been attributed to dye desorption.[33] Such a dye detachment or a weakening of dye bonding causes an increase in the oxygen vacancy concentration at the TiO_2 surface, resulting in a structure behavior similar to an unsensitized TiO_2 film (like the base photoanode), as has been observed for the photoanode of our DSSCs prepared with a 40 vol % water-containing electrolyte.

Figure 4 shows the variation of interatomic distances for the first six atoms around the central/absorbing Ti atom of TiO_2 in the electrolyte-exposed photoanodes. Figure 4B presents the same results as that of Figure 4A, however, with different *Y*-axis scales to depict the variations with more clarity. Comparing the atomic positions in the base sample with those of the model, we can make the following conclusions (see Table 2). First, the variations of interatomic distances for the @O1.1 and @Ti2.1 atom in all of the samples are insignificant, as the values fall within the error bars. However, the variations of interatomic distances for @O1.2, @O2.1, @Ti1.1, and @O2.2 atoms are significant. While the distance corresponding to the @O2.1 and @O2.2 atoms decreases, it increases for the @O1.2 and @Ti1.1 atoms. On the other hand, for all of the samples, the interatomic distance for the @Ti1.2 atom does not suffer any significant change, as all of the values fall within the error bars.

https://doi.org/10.1021/acsaem.2c00245
ACS Appl. Energy Mater. 2022, 5, 4817−4828

In the case of the photoanode exposed to a 0 vol % water-containing electrolyte, the interatomic distances for all of the considered atoms remain close to their values in the model (bulk-like structure), indicating that dye-adsorbed TiO_2 in the anode remained relaxed after being exposed to the electrolyte. The result also confirms the fact that the dye molecules occupy most of the oxygen vacancy sites of the metal oxide surface.

The effects of the presence of an electrolyte and dye in the TiO_2 film structure emerge on comparing the results of the photoanode exposed to a 0 vol % water-containing electrolyte with the base film (see Table 2). The interatomic distances for the @O1.1 and @Ti2.1 atoms show insignificant variation as they fall into the error bars. A careful analysis of the interatomic distances enlisted in Table 2 will reveal that the interatomic distances for the @O1.2 and @Ti1.1 atoms in the photoanode decreased slightly, while the values for the @O2.1 and @O2.2 atoms increased marginally. Such a variation in interatomic distances of these atoms might be the result of the presence of electronegative elements such as nitrogen (present in the acetonitrile solvent) or oxygen (dissolved in the electrolyte solution), which try to occupy the oxygen vacancy sites of the TiO_2 surface. In fact, occupation of oxygen vacancy sites by nitrogen atoms has been observed by Daraee et al.,[35] who reported a change in the band-gap energy of TiO_2 films due to nitrogen doping. Occupation of oxygen vacancy sites by nitrogen atoms has also been observed by Gartner et al.[36] in their multilayered porous TiO_2 films prepared by dip coating. By analyzing their ammonia-annealed TiO_2 films by X-ray diffraction (XRD) and X-ray photoelectron spectroscopy (XPS), they showed that nitrogen atoms can be easily incorporated into the TiO_2 surface, occupying the anion positions. They also showed that OH groups (present in water) can interact with the TiO_2 crystal lattice. On the other hand, Zhu et al.[37] utilized TiO_2 photoanodes in different electrolyte solvents with distinct concentrations of OH groups to study the stability of the semiconductor. Although they did not provide the mechanism of solvent interaction with the TiO_2 surface during the operation of DSSCs, the obtained results clearly evidence the possibility of strong interaction between the electrolyte solvents and the TiO_2 surface in contact, depending on the nature of the former.

In the case of a TiO_2 photoanode exposed to a 5 vol % water content electrolyte, the interatomic distances corresponding to the @O1.2, @Ti1.1, and @Ti2.1 atoms do not change significantly when they are compared with the photoanode exposed to a 0 vol % water-containing electrolyte. In fact, the variations lie within the fluctuation limit or the error bars. On the other hand, the interatomic distance for the @O1.1, @O2.1, and @O2.2 atoms changes significantly. While for the @O2.1 and @O1.1 atoms, the interatomic distance reduces, indicating the formation of a compressed lattice, the interatomic distance for the @O2.2 atom increases, representing its more relaxed state. The results clearly indicate that the H_2O molecules have a strong influence on the structure of the TiO_2 lattice, in accordance with our hypothesis.

Finally, for the photoanode exposed to the 40 vol % water-containing electrolyte, all of the studied interatomic distances take the values comparable to those of the base film (Figure 4B and Table 2). As the base film was not sensitized, neither ever been in contact with the electrolyte solution, a similar lattice parameter of the TiO_2 photoanode exposed to the 40 vol % water-containing electrolyte clearly indicates that its surface becomes dye-free on exposure with the electrolyte. Therefore, the dye adsorption capacity of the TiO_2 photoanode surface is lost by exposing it to the electrolyte with 40 vol % water. In other words, water molecules compete for the oxygen vacancies at the TiO_2 surface and desorb or weaken the bond of the attached dye molecules, leading to a decrease in the DSSC short-circuit photocurrent density, in agreement with previously reported works.[12,14,15]

The Debye−Waller factor (σ_j^2) is a structure parameter that is related to atomistic disorder in a crystalline lattice of materials. In the case of TiO_2, the σ_j^2 represents the static or thermal disorder in the lattice due to sample pretreatment or when XAFS measurements are performed at different temperatures. As all of the XAFS measurements in this study were performed at a fixed (room) temperature, and hence there occurred no thermal vibrations variations, consequently, all of the variations in σ_j^2 can be considered as a static disorder. Also, as the reference model (ideal bulk-like TiO_2 structure) does not contain lattice disorder, the corresponding σ_j^2 is zero for all of the six studied atoms (Figure 3). Figure 5A,B presents σ_j^2 values for all of the data displayed in Figure 2. A first observation is that σ_j^2 falls within the allowed value range (0.002−0.03 Å^2). As shown in Figure 5A, the σ_j^2 value for the @O2.2 atom for all of the photoanodes is the most affected one due to water incorporation in the electrolyte. The higher σ_j^2 value in comparison with the other studied atoms indicates a higher degree of static disorder. On the other hand, the least affected atoms of the TiO_2 lattice are the @O1.1 and @O2.1 atoms with the smallest values of σ_j^2.

From the results presented in Figure 5B and Table 3, we can observe some general features regarding the variations of σ_j^2 in the studied atoms. First, we observe that after dye adsorption and after being in contact with the electrolyte solution (with no water), the TiO_2 film shows a more disordered lattice, as noticed by the highest values of σ_j^2 for all of the studied atoms when compared with the base film. Correlating this observation with the results presented in Figure 4, we can conclude that the solvents used in the standard electrolyte and the attached dye molecules onto the TiO_2 surface play important roles in modifying the structural and electronic properties of the semiconductor. Second, incorporation of 5 vol % water in the electrolyte solution reduces the structural disorder in TiO_2, with a minimum variation of the interatomic distance for all of the studied atoms apart from the @Ti2.1 atom. As shown in Table 3, the σ_j^2 values for these specific atoms are lower, even than the base film. These results indicate that the addition of water keeps the electrolyte molecules away from the TiO_2 surface and the interaction between the superficial Ti atoms of the semiconductor and the water molecules becomes stronger. The strong interaction between the Ti atoms of the TiO_2 lattice and water molecules in the electrolyte facilitates the incorporation of oxygen atoms in the TiO_2 network. Several research groups have observed similar effects when small atoms are in contact with TiO_2. For example, Qu and Meyer[38] studied the effect of small cations such as H^+ and Li^+ at the TiO_2−electrolyte interface, observing a rapid and efficient intermolecular charge transfer across the nanocrystalline surface. On the other hand, Shultz et al.[39] studied the mechanisms of water interaction with the semiconductor surface by sum-frequency generation (SFG) vibrational spectroscopy. They found that water adsorbed on the TiO_2 surface produces broad SFG peaks due to hydrogen bonding. Our results are in good accordance with the observations of Shultz et al., reinforcing the idea that water

https://doi.org/10.1021/acsaem.2c00245
ACS Appl. Energy Mater. 2022, 5, 4817−4828

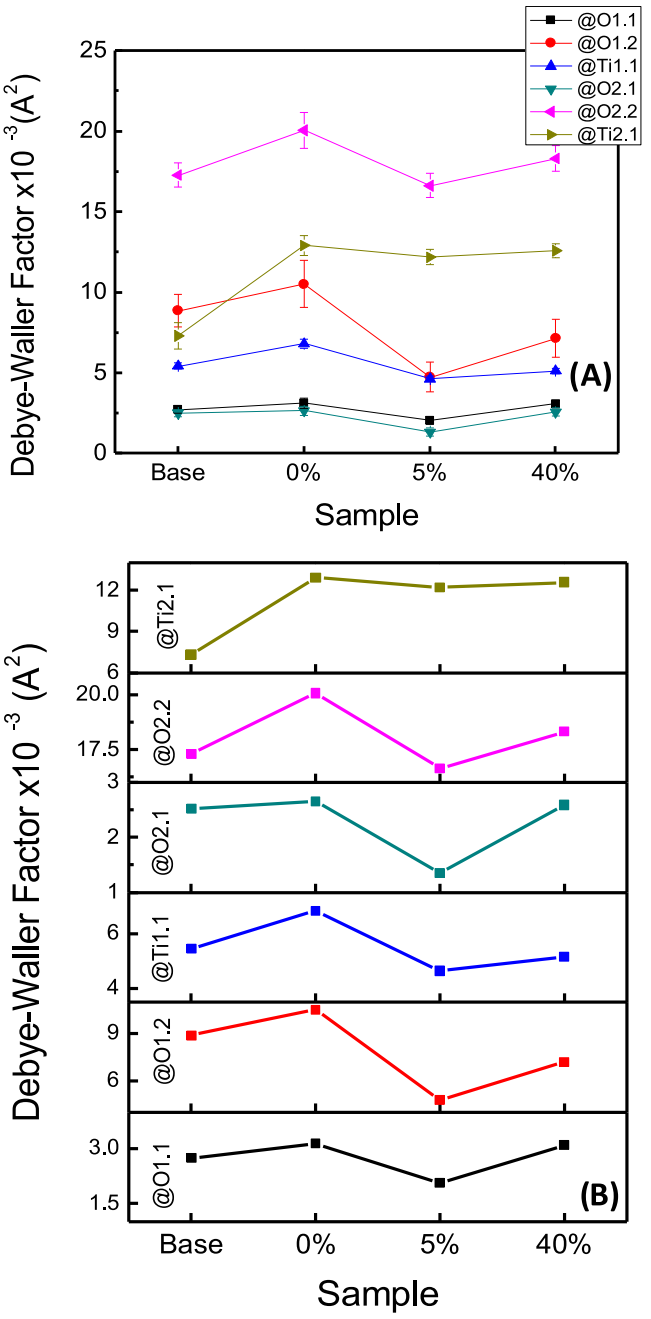

Figure 5. Debye–Waller factor variations for the first six atoms in the TiO_2 lattice of different photoanodes measured in this study. (A) All of the data in the same plot and (B) same data as in (A) presented in a stack for individual analysis.

Table 3. Summary of the Debye–Waller Factor for the Water-Exposed Photoanodes

	Debye–Waller factor ($\times 10^{-3}$ Å^2)					
sample	@O1.1	@O1.2	@Ti1.1	@O2.1	@O2.2	@Ti2.1
base	2.74	8.87	5.45	2.52	17.3	7.32
0%	3.14	10.53	6.83	2.66	20.07	12.92
5%	2.06	4.75	4.64	1.35	16.64	12.2
40%	3.09	7.17	5.15	2.59	18.32	12.59

interacts strongly with the metal oxide surface, leading to its structure modification.

The third and final significant feature was noticed for the photoanode exposed to the 40 vol % water content electrolyte. In this case, the σ_j^2 value for all of the studied atoms increased, indicating the formation of a more disordered lattice in comparison to the case of the photoanode exposed to a 5 vol % water-containing electrolyte. This result reinforces the hypothesis that water incorporated in larger quantities (higher than 5 vol %) weakens the bonding of dye molecules with the TiO_2 surface, creating a TiO_2 lattice disorder like the base film. Sumita et al.[40] theoretically investigated the structural and electronic properties of the liquid acetonitrile/anatase ((ACN)/TiO_2) interface involving water molecules to analyze the effect of water contamination in the typical electrolyte solution on the stability of DSSC through density functional molecular dynamics simulations at room temperature. They described how the ACN is strongly adsorbed onto the TiO_2 surface due to the back-donating effect, which induces a decrease in the TiO_2 band gap. An interesting conclusion they draw was that it is impossible for ACN molecules to fully cover the metal oxide surface, leaving a lot of available TiO_2 surface for water to dive on the TiO_2 oxygen sites. The same report explains that the water molecules adsorbed over the TiO_2 surface before its contact with the ACN solvent are hard to remove due to the strong interaction between H (from water) and O atoms (from TiO_2), suggesting that water manifests a stronger interaction with the TiO_2 surface than the ACN molecules. Finally, the investigation highlights the possibility for water to become a cation radical by capturing a hole generated by irradiation, which can attack the dye molecules adsorbed on the TiO_2 surface and produce undesired effects. All of these results support our hypothesis that the interaction of water molecules with the TiO_2 surface is stronger than their interaction with the solvent molecules in the electrolyte solution and the dye molecules, leading to a dye detachment or weakening of dye bonding at the surface of the TiO_2 photoanode.

3.3. Electrodynamic Characterization. In this section, we will present the link between the observed structural changes of the TiO_2 photoanodes and the electrodynamic and photovoltaic parameters of the assembled DSSCs due to the addition of water in the electrolyte solution. Wang et al.[34] studied the shift of the TiO_2 conduction band edge induced by the adsorption of Z907 dye molecules on their surface. Using electrochemical impedance spectroscopy (similar to SLITM), they have shown that the conduction band of a dye-grafted TiO_2 electrode moves downward compared with that of a bare TiO_2 electrode (without dye), both in assembled DSSCs with the same electrolyte. Such a downward shift of the conduction band edge due to adsorption of dye molecules at the TiO_2 surface might also be related to the structural changes (presented in Section 3.2) and the filling of oxygen vacancies at the TiO_2 surface, as have been discussed earlier. With the increase of adsorbed dye molecules, the concentration of oxygen vacancies at the surface of the TiO_2 photoanode will decrease, and its conduction band would shift to lower energy (downward shift). In this sense, we can establish a direct relationship between the downward conduction band shifts and the variations of interatomic distances. For instance, by comparing the @O2.2 atom of the photoanode exposed to a 0 vol % water content electrolyte and base film (Figure 4B).

It is important to mention that in our experiments, the base film was not exposed to the electrolyte solution and we are

https://doi.org/10.1021/acsaem.2c00245
ACS Appl. Energy Mater. 2022, 5, 4817–4828

assuming that the electrolyte solution does not play an important role in the TiO_2 conduction band shift.

From the results presented in Figure 5, it seems that the dye adsorption and the presence of an electrolyte generate more lattice disorder at the surface of the TiO_2 photoanode. From the photovoltaic results presented in Section 3.1, we can see that adding 5 vol % of water in the electrolyte solution improves the overall performance (efficiency) of DSSCs due to an increase in the short-circuit current. An increase in the interatomic distance in the TiO_2 layer on utilizing DSSCs containing 0 and 5 vol % water in electrolyte solutions (Figure 4 and Table 2) probably causes a downward shift of the TiO_2 conduction band, and consequently, an increase in the J_{SC} due to the improvement of electron injection efficiency. Based on this assumption, we expect that for the cells fabricated with higher water content (10−40 vol %) electrolytes, the efficiency should decrease, as the J_{SC} would fall due to the decrease in the interatomic distance between the @O2.2 atoms and the scattering Ti atom (Figure 4), in agreement with our experimental results shown in Table 1.

On the other hand, as shown in Figure 1C, the V_{OC} of the assembled DSSCs decreases with the increase in water content in the electrolyte. This result could be explained by considering a downward shift of the TiO_2 conduction band, as has been reported by Kopidakis and co-workers.[41] Band-edge movement occurs when enough negative or positive charges (or dipoles) build up at the surface of the TiO_2 film, inducing a change in the potential of their Helmholtz layer. A negative surface charge build-up can cause the edges to shift upward, toward negative electrochemical potential, leading to a higher V_{OC}. In contrast, a positive surface charge build-up (as occurs for water molecules at the TiO_2 surface) can cause the conduction band edge to move downward, toward positive potential, leading to a lower V_{OC}.[20,23,42] This occurs if the total density of energy states within the TiO_2 band gap do not change. To determine the contribution of water added to the electrolyte solution on the band-edge shift of DSSC photoanodes, we performed electrodynamic characterizations of the DSSCs fabricated with electrolytes containing different water contents through stepped light-induced transient measurements (SLITM). The movement of the quasi-Fermi level (or conduction band edge) of TiO_2 electrodes in DSSCs was determined through the V_{OC} vs electron charge density (n) plots,[42] as shown in Figure 6. As indicated with a red arrow, at a fixed electron charge density of about 10^{17} cm^{-3}, the addition of 5 vol % water in the electrolyte leads to a downward shift of the TiO_2 quasi-Fermi level by about 100 mV. When a band-edge movement occurs downward, the energy difference between the lowest unoccupied molecular orbital (LUMO) of the dye and the TiO_2 conduction band edge increases, leading to an increase in electron injection efficiency. The increase in electron injection efficiency causes an increase in the J_{SC} of the DSSC fabricated with the electrolyte containing 5 vol % water (in comparison with the reference DSSC, which contains no water). Finally, the variations of J_{SC} and V_{OC} in an inverse manner (i.e., an increase of J_{SC} and a decrease of V_{OC} with the addition of 5 vol % water in the electrolyte) can be explained in terms of a downward shift of the TiO_2 quasi-Fermi level (or the conduction band), in congruence with the hypothesis we considered. The filling of oxygen vacancies at the TiO_2 surface is directly related to the downward shift of the semiconductor quasi-Fermi level. However, such a band-edge movement analysis cannot be applied to the DSSC fabricated with a 40 vol % water-containing electrolyte (blue circles in Figure 6) due to a significant change in the variation of charge density with voltage compared with the reference one (nonlinear trend of the semilogarithmic V_{OC} versus n plot). However, assuming a similar slope as of the reference DSSC, an upward shift of quasi-Fermi level is expected for the TiO_2 photoanode utilized in the DSSC fabricated with 40 vol % water content, decreasing both J_{SC} and V_{OC} for the DSSC. The change of the slope for the DSSC fabricated with a 40 vol % water content electrolyte observed in Figure 6 (an increase by about 60%) can be related to the variation of two electronic properties of the TiO_2 electrode due to water incorporation: (1) the variation in the total electron trap density and (2) the variation in their distribution within the TiO_2 band gap.[42−44] Several authors have also reported the effect of water in the electrolyte on the band-edge movement of a semiconducting photoanode and the corresponding electrodynamical behaviors of DSSCs. For instance, Frank et al.[15] found that adding water to the electrolyte solution strongly alters the energy level alignments of TiO_2, retarding charge carrier recombination at the electrode/redox-electrolyte interface and increasing the dark exchange current density. Increases in the photocurrent density and an enhancement of efficiency of solar cells have also been observed.

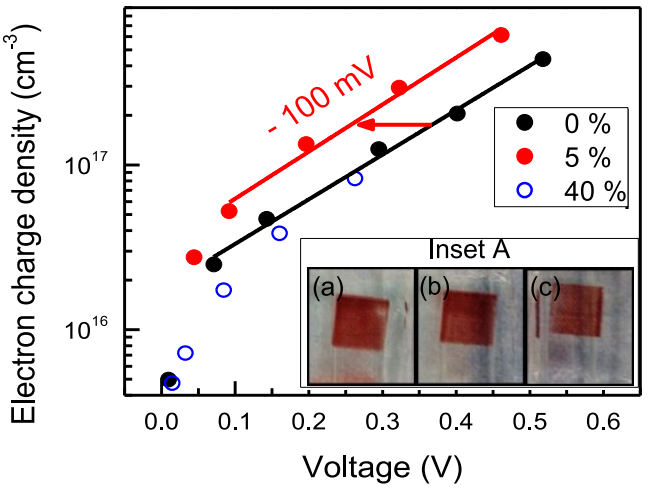

Figure 6. Electron charge density vs open-circuit voltage plots for the DSSC assemblies without and with different % of water volume in the electrolyte solution. Straight lines correspond to the best fits to the experimental data points, which follow an exponential distribution of electronic states (traps) within the TiO_2 band gap. Inset A shows the optical images of the photoanodes after their use in DSSCs fabricated using (a) 0%, (b) 5%, and (c) 40% water content electrolytes.

According to our hypothesis (filling of oxygen vacancies with dye or water molecules), a decrease in the total trap density (N) is also expected at the surface of the TiO_2 photoanode while utilizing a 5 vol % water-containing electrolyte due to oxygen vacancy filling. To verify this, we calculated the variation of N (total trap density) in the TiO_2 surface following a previously reported procedure.[23] The ratio of trap densities in the reference electrode N_{ref} (in this case, the 0 vol % water photoanode) and the electrode containing water molecules N (in the case of 5 vol % water photoanode) can be expressed as

$$\frac{N_{ref}}{N} = \left(\frac{D}{D_{ref}}\right)^{\alpha} \quad (3)$$

https://doi.org/10.1021/acsaem.2c00245
ACS Appl. Energy Mater. 2022, 5, 4817−4828

where D and D_{ref} are the, respective, electron diffusion coefficients for the 5 vol % water-containing electrolyte and the reference DSSC photoanode at the same electron charge density, respectively, and α is the average depth of an exponential trap distribution.[20−23] The electron charge density n in terms of V_{OC} can be expressed as

$$n \sim N \exp\left\{\frac{\alpha V_{OC}}{kT}\right\} \quad (4)$$

where k and T are the Boltzmann constant and temperature, respectively. Equation 4 was used to fit the experimental data for the DSSCs fabricated with 0 and 5 vol % water-containing electrolytes (Figure 6), which produced an average value of 0.1228 for α. In Figure 7, we plot the electron diffusion coefficients for the DSSC electrodes fabricated with 0, 5, and 40 vol % water-containing electrolytes as a function of electron charge density, obtained by SLITM, as described in the experimental section. As indicated by a green arrow, at a fixed electron charge density (around 10^{17} cm^{-3}), the electron diffusion coefficient for the DSSC fabricated with 5 vol % water-containing electrolyte is about 1.57 times of the electron diffusion coefficient in the reference DSSC.

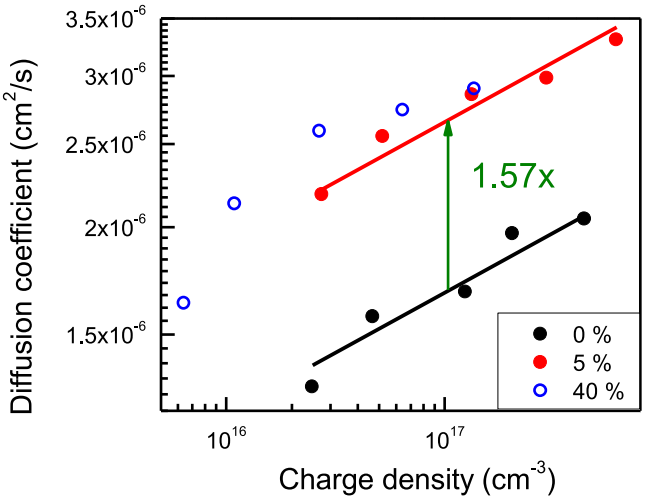

Figure 7. Diffusion coefficient vs charge density plots for the DSSCs fabricated with electrolytes containing different amounts of water. Straight lines correspond to the best fits to the experimental data points, which follow a power-law dependence of the diffusion coefficient with electron charge density.

By incorporating the values of $\alpha = 0.1228$ and $D/D_{ref} = 1.57$ in eq 3, we obtained the value of $N_{ref}/N = 1.056$, which indicates about a 6% decrease in the total trap density at the photoanode surface on utilizing a 5 vol % water-containing electrolyte in the device. The result supports our hypothesis that the presence of water in the electrolyte decreases the concentration of oxygen vacancies (trap states) at the TiO_2 photoanode surface, causing an increase in the interatomic distance between the @O2.2 atoms of the TiO_2 lattice. Nevertheless, as this is the first work that correlates the fine structure of a semiconductor photoanode and electrodynamic behaviors of DSSC assembled with different water-containing electrolytes, further experimental and theoretical studies are required to establish the considered assumption firmly.

4. CONCLUSIONS

From the findings of the present study, we can conclude that in comparison to the nonwater-added DSSC, adding 5 vol % of water in a normal electrolyte solution boosts the total efficiency of DSSCs by about 14%. The key factor that contributes to the efficiency gain is the J_{SC}, which increases by about 18.6% with respect to the current density of the reference device. The addition of water in the electrolyte solution causes a progressive reduction in V_{OC}. The variation in V_{OC} is linked to the downward shift (toward positive potential) of the TiO_2 band edge. At the same time, the increase of J_{SC} in the DSSCs fabricated with 5 vol % water-containing electrolyte is due to a downward shift of the conduction band edge, which causes an increase in electron injection efficiency of the dye. The connection between these findings and structural variations is based on the incorporation of oxygen from water into TiO_2 oxygen vacancies, leaving hydrogen atoms exposed on their surface, which results in a band-edge shift toward more positive potentials due to positive charge accumulation at the TiO_2 surface. As a result of water incorporation into the oxygen vacancies, the total trap density decreases, increasing the diffusion coefficient of water-exposed photoanodes. Finally, for the most efficient system, this is translated into a less static disordered (lowest Debye−Waller values) and more relaxed lattice (interatomic distances comparable to the bulk-like TiO_2). On the other hand, a more static disordered (high Debye−Waller values compared to the most efficient system) and less relaxed lattice (lowest interatomic distances compared to the bulk-like TiO_2) were seen at the maximum water % (40 vol % in the present study) in the electrolyte solution. Such changes in the TiO_2 lattice cause a drastic reduction in the short-circuit photocurrent of the fabricated DSSC, owing to dye separation or a weak dye attachment at the TiO_2 surface. While the results obtained in this study are useful for understanding the interaction of water molecules with a TiO_2 photoanode and the fabrication of stable, environmentally friendly DSSCs, the findings can also be utilized for studying nanostructured TiO_2 films for other applications, which have not yet been explored, for example, for the understanding about the process that leads to the dye degradation at the semiconductor surface, to innovate and improve the process to avoid water incorporation onto the TiO_2 surface, and/or to incorporate water in the electrolyte solutions to get ecofriendly devices.

AUTHOR INFORMATION

Corresponding Authors

Alfredo Romero-Contreras − *Instituto de Física, Benemérita Universidad Autónoma de Puebla, Puebla, Puebla 72570, México;* orcid.org/0000-0001-6861-7486; Email: aromero@ifuap.buap.mx

Julio Villanueva-Cab − *Instituto de Física, Benemérita Universidad Autónoma de Puebla, Puebla, Puebla 72570, México;* orcid.org/0000-0002-6261-9197; Email: juliovc@ifuap.buap.mx

Authors

Juan S. Lezama Pacheco − *Department of Earth System Science, Stanford University, Stanford, California 94305, United States*

Joaquin Alvarado − *Benemérita Universidad Autónoma de Puebla, CIDS, Puebla, Puebla 72000, México*

https://doi.org/10.1021/acsaem.2c00245
ACS Appl. Energy Mater. 2022, 5, 4817−4828

Umapada Pal − *Instituto de Física, Benemérita Universidad Autónoma de Puebla, Puebla, Puebla 72570, México;* orcid.org/0000-0002-5665-106X

Complete contact information is available at: https://pubs.acs.org/10.1021/acsaem.2c00245

Funding

CONACyT (grant CB-2015-01-256946 and CB-A1-S-26720) and FORDECYT-PRONACES (grant CF-2019-848260). University of California Institute for Mexico and the United States (UC MEXUS) and CONACyT (grant #CN-17-14).

Notes

The authors declare no competing financial interest.

■ ACKNOWLEDGMENTS

The authors gratefully acknowledge the Consejo Nacional de Ciencia y Tecnología (CONACyT), Mexico, and VIEP-BUAP, Mexico, for financial support. They especially thank the SLAC National Accelerator Laboratory, Stanford University, for facilities access and experimental support.

■ REFERENCES

(1) Photovoltaic Research, NREL. Best Research-Cell Efficiency Chart. https://www.nrel.gov/pv/cell-efficiency.html (accessed Dec, 2021).

(2) Mathew, S.; Yella, A.; Gao, P.; Humphry-Baker, R.; Curchod, B. F.; Ashari-Astani, N.; Grätzel, M.; et al. Dye-sensitized solar cells with 13% efficiency achieved through the molecular engineering of porphyrin sensitizers. *Nat. Chem.* **2014**, *6*, 242−247.

(3) Gong, J.; Sumathy, K.; Qiao, Q.; Zhou, Z. Review on dye-sensitized solar cells (DSSCs): Advanced techniques and research trends. *Renewable Sustainable Energy Rev.* **2017**, *68*, 234−246.

(4) Sonigara, K. K.; Vaghasiya, J. V.; Machhi, H. K.; Prasad, J.; Gibaud, A.; Soni, S. S. Anisotropic One-Dimensional Aqueous Polymer Gel Electrolyte for Photoelectrochemical Devices: Improvement in Hydrophobic TiO_2−Dye/Electrolyte Interface. *ACS Appl. Energy Mater.* **2018**, *1*, 3665−3673.

(5) Fagiolari, L.; Bonomo, M.; Cognetti, A.; Meligrana, G.; Gerbaldi, C.; Barolo, C.; Bella, F. Photoanodes for Aqueous Solar Cells: Exploring Additives and Formulations Starting from a Commercial TiO_2 Paste. *ChemSusChem* **2020**, *13*, 6562−6573.

(6) Kim, J. H.; Park, S. Y.; Lim, D. H.; Lim, S. Y.; Choi, J.; Koo, H. J. Eco-Friendly Dye-Sensitized Solar Cells Based on Water-Electrolytes and Chlorophyll. *Materials* **2021**, *14*, No. 2150.

(7) Jilakian, M.; Ghaddar, T. H. Eco-Friendly Aqueous Dye-Sensitized Solar Cell with a Copper(I/II) Electrolyte System: Efficient Performance under Ambient Light Conditions. *ACS Appl. Energy Mater.* **2022**, *5*, 257−265.

(8) Galliano, S.; Bella, F.; Bonomo, M.; Viscardi, G.; Gerbaldi, C.; Boschloo, G.; Barolo, C. Hydrogel Electrolytes Based on Xanthan Gum: Green Route towards Stable Dye-Sensitized Solar Cells. *Nanomaterials* **2020**, *10*, No. 1585.

(9) Galliano, S.; Bella, F.; Gerbaldi, C.; Falco, M.; Viscardi, G.; Grätzel, M.; Barolo, C. Photoanode/Electrolyte Interface Stability in Aqueous Dye-Sensitized Solar Cells. *Energy Technol.* **2017**, *5*, 300−311.

(10) Tropsha, Y. G.; Harvey, N. G. Activated Rate Theory Treatment of Oxygen and Water Transport through Silicon Oxide/Poly(ethylene terephthalate) Composite Barrier Structures. *J. Phys. Chem. B* **1997**, *101*, 2259−2266.

(11) Park, J.; Lee, P.; Ko, M. J. Design and Fabrication of Long-Term Stable Dye-Sensitized Solar Cells: Effect of Water Contents in Electrolytes on the Performance. *Int. J. Precis. Eng. Manuf.-Green Technol.* **2019**, *6*, 125−131.

(12) Liu, Y.; Hagfeldt, A.; Xiao, X.-R.; Lindquist, S.-E. Investigation of influence of redox species on the interfacial energetics of a Dye-Sensitized nanoporous TiO_2 solar cell. *Sol. Energy Mater. Sol. Cells* **1998**, *55*, 267−281.

(13) Glinka, A.; Gierszewski, M.; Ziółek, M. Effects of Aqueous Electrolyte, Active Layer Thickness and Bias Irradiation on Charge Transfer Rates in Solar Cells Sensitized with Top Efficient Carbazole Dyes. *J. Phys. Chem. C* **2018**, *122*, 8147−8158.

(14) Law, C. H.; Pathirana, S. C.; Li, X.; Anderson, A. Y.; Barnes, P. R. F.; Listorti, A.; Ghaddar, T. H.; O'Regan, B. C. Water-Based Electrolytes for Dye-Sensitized Solar Cells. *Adv. Mater.* **2010**, *22*, 4505−4509.

(15) Zhu, K.; Jang, S.-R.; Frank, A. J. Effects of water intrusion on the charge-carrier dynamics, performance, and stability of dye-sensitized solar cells. *Energy Environ. Sci.* **2012**, *5*, 9492.

(16) Hui, Z.; Xiong, Y.; Heng, L.; Yuan, L.; Yu-Xiang, W. Explanation of Effect of Added Water on Dye-Sensitized Nanocrystalline TiO 2 Solar Cell: Correlation between Performance and Carrier Relaxation Kinetics. *Chin. Phys. Lett.* **2007**, *24*, 3272−3275.

(17) Yan, W.; Huo, M.-M.; Hu, R.; Wang, Y. Working area effects on the energetic distribution of trap states and charge dynamics of dye-sensitized solar cells. *RSC Adv.* **2019**, *9*, 1734−1740.

(18) Yeoh, M. E.; Jaloman, A.; Chan, K. Y. Aging effect in dye-sensitized solar cells sealed with thermoplastic films. *Microelectronics International* **2019**, *36*, 68−72.

(19) Michael Kelzenberg. Software. http://mkelzenb.caltech.edu/software.html (accessed June, 2019).

(20) Villanueva-Cab, J.; Montaño-Priede, J. L.; Pal, U. Effects of Plasmonic Nanoparticle Incorporation on Electrodynamics and Photovoltaic Performance of Dye Sensitized Solar Cells. *J. Phys. Chem. C* **2016**, *120*, 10129−10136.

(21) Nakade, S.; Kanzaki, T.; Wada, Y.; Yanagida, S. Stepped Light-Induced Transient Measurements of Photocurrent and Voltage in Dye-Sensitized Solar Cells: Application for Highly Viscous Electrolyte Systems. *Langmuir* **2005**, *21*, 10803−10807.

(22) van de Lagemaat, J.; Frank, A. J. Nonthermalized Electron Transport in Dye-Sensitized Nanocrystalline TiO2 Films: Transient Photocurrent and Random-Walk Modeling Studies. *J. Phys. Chem. B* **2001**, *105*, 11194−11205.

(23) Rodríguez-Perez, M.; Noh-Pat, F.; Romero-Contreras, A.; Reyes-Ramírez, E. J.; Krishnan, S. K.; Ortíz-Quiñonez, J. L.; Alvarado, J.; Pal, U.; Olalde-Velasco, P.; Villanueva-Cab, J.). Re-evaluating the role of phosphinic acid (DINHOP) adsorption at the photoanode surface in the performance of dye-sensitized solar cells. *Phys. Chem. Chem. Phys.* **2020**, *22*, 1756−1766.

(24) Ravel, B.; Newville, M. ATHENA, ARTEMIS, HEPHAESTUS: data analysis for X-ray absorption spectroscopy using IFEFFIT. *J. Synchrotron Radiat.* **2005**, *12*, 537−541.

(25) The FEFF Project. http://feff.phys.washington.edu/ (accessed June, 2020).

(26) Calvin, S. *XAFS for Everyone* (Illustrated ed.). CRC Press, 2013.

(27) van Bokhoven, J. A.; Lamberti, C.; van Bokhoven, J. A. *X-Ray Absorption and X-Ray Emission Spectroscopy*; Wiley: Hoboken, NJ, United States, 2016.

(28) Ruiz-Lopez, M. F.; Munoz-Paez, A. A theoretical study of the XANES spectra of rutile and anatase. *J. Phys.: Condens. Matter* **1991**, *3*, 8981−8990.

(29) Darapaneni, P.; Meyer, A. M.; Sereda, M.; Bruner, A.; Dorman, J. A.; Lopata, K. Simulated field-modulated X-ray absorption in titania. *J. Chem. Phys.* **2020**, *153*, No. 054110.

(30) Rutley, F. *Rock-Forming Minerals*; Leopold Classic Library: London, U.K., 2016.

(31) Austin, R. H.; Lim, S. F. The Sackler Colloquium on promises and perils in nanotechnology for medicine. *Proc. Natl. Acad. Sci. U.S.A.* **2008**, *105*, 17217−17221.

(32) Schliesser, J. M.; Smith, S. J.; Li, G.; Li, L.; Walker, T. F.; Parry, T.; Boerio-Goates, J.; Woodfield, B. F. Heat capacity and thermodynamic functions of nano-TiO_2 anatase in relation to bulk-TiO_2 anatase. *J. Chem. Thermodyn.* **2015**, *81*, 298−310.

(33) Wang, M.; Li, X.; Lin, H.; Pechy, P.; Zakeeruddin, S. M.; Grätzel, M. Passivation of nanocrystalline TiO_2 junctions by surface

adsorbed phosphinate amphiphiles enhances the photovoltaic performance of dye sensitized solar cells. *Dalton Trans.* **2009**, *45*, 10015.
(34) Zhang, X. T.; Taguchi, T.; Wang, H. B.; Meng, Q. B.; Sato, O.; Fujishima, A. Investigation of the stability of solid-state dye-sensitized solar cells. *Res. Chem. Intermed.* **2007**, *33*, 5−11.
(35) Daraee, M.; Ghasemy, E.; Rashidi, A. Effective adsorption of hydrogen sulfide by intercalation of TiO2 and N-doped TiO2 in graphene oxide. *J. Environ. Chem. Eng.* **2020**, *8*, No. 103836.
(36) Gartner, M.; Osiceanu, P.; Anastasescu, M.; Stoica, T.; Stoica, T. F.; Trapalis, C.; Giannakopoulou, T.; Todorova, N.; Lagoyannis, A. Investigation on the nitrogen doping of multilayered, porous TiO_2 thin films. *Thin Solid Films* **2008**, *516*, 8184−8189.
(37) Zhu, K.; Neale, N. R.; Halverson, A. F.; Kim, J. Y.; Frank, A. J. Effects of Annealing Temperature on the Charge-Collection and Light-Harvesting Properties of TiO_2 Nanotube-Based Dye-Sensitized Solar Cells. *J. Phys. Chem. C* **2010**, *114*, 13433−13441.
(38) Qu, P.; Meyer, G. J. Proton-Controlled Electron Injection from Molecular Excited States to the Empty States in Nanocrystalline TiO_2. *Langmuir* **2001**, *17*, 6720−6728.
(39) Wang, C.; Groenzin, H.; Shultz, M. J. Comparative Study of Acetic Acid, Methanol, and Water Adsorbed on Anatase TiO_2 Probed by Sum Frequency Generation Spectroscopy. *J. Am. Chem. Soc.* **2005**, *127*, 9736−9744.
(40) Sumita, M.; Sodeyama, K.; Han, L.; Tateyama, Y. Water Contamination Effect on Liquid Acetonitrile/TiO2 Anatase (101) Interface for Durable Dye-Sensitized Solar Cell. *J. Phys. Chem. C* **2011**, *115*, 19849−19855.
(41) Kopidakis, N.; Neale, N. R.; Frank, A. J. Effect of an Adsorbent on Recombination and Band-Edge Movement in Dye-Sensitized TiO_2 Solar Cells: Evidence for Surface Passivation. *J. Phys. Chem. B* **2006**, *110*, 12485−12489.
(42) Villanueva-Cab, J.; Jang, S. R.; Halverson, A. F.; Zhu, K.; Frank, A. J. Trap-Free Transport in Ordered and Disordered TiO_2 Nanostructures. *Nano Lett.* **2014**, *14*, 2305−2309.
(43) Wang, K.-P.; Teng, H. Structure-intact TiO_2 nanoparticles for efficient electron transport in dye-sensitized solar cells. *Appl. Phys. Lett.* **2007**, *91*, No. 173102.
(44) Kopidakis, N.; Neale, N. R.; Zhu, K.; van de Lagemaat, J.; Frank, A. J. Spatial location of transport-limiting traps in TiO2 nanoparticle films in dye-sensitized solar cells. *Appl. Phys. Lett.* **2005**, *87*, No. 202106.

https://doi.org/10.1021/acsaem.2c00245
ACS Appl. Energy Mater. 2022, 5, 4817−4828